Relaxation processes in an epoxy resin studied by time-resolved optical Kerr effect

D. Prevosto,[1] P. Bartolini,[2,3] R. Torre,[2,3,4] M. Ricci,[2,3,5] A. Taschin,[2,3,4] S. Capaccioli,[1] M. Lucchesi,[1] P. Rolla[1]
[1]*Dipartimento di Fisica, Università di Pisa, and INFM, Unità di Pisa, via F. Buonarroti 2, I-56127, Pisa, Italy*
[2]*LENS, Polo Scientifico, Università di Firenze, via N. Carrara 1, 50019 Sesto Fiorentino, Italy*
[3]*INFM, Unità di Firenze, via G. Sansone 1, 50019 Sesto Fiorentino, Italy*
[4]*Dipartimento di Fisica, Polo Scientifico, Università di Firenze, via G. Sansone 1, 50019 Sesto Fiorentino, Italy*
[5]*Dipartimento di Chimica Fisica, Università della Basilicata, via N. Sauro 85, Potenza, Italy*
(Received 7 February 2002; published 29 July 2002)

The dynamics of the epoxy resin phenyl glycidyl ether, a fragile glass-forming liquid, is investigated in the liquid and supercooled phases by time-resolved optical Kerr effect experiment with an heterodyne detection technique. We tested the mode-coupling theory and found that the predicted dynamic scenario allows to reproduce properly the measured signal, for $t>1$ ps, in the whole temperature interval investigated. Furthermore, the values of T_c and λ, obtained from the analysis of three different and independent dynamic regimes (α regime, von Schweidler, β regime), are in remarkable agreement. Moreover, relaxation times obtained from optical Kerr effect and dielectric spectroscopy measurements are compared. The two time scales differ only for a constant factor in the whole temperature interval investigated.

DOI: 10.1103/PhysRevE.66.011502 PACS number(s): 64.70.Pf, 78.20.Jq, 78.47.+p

I. INTRODUCTION

Glass-forming systems can be supercooled below the melting temperature in a metastable liquid phase without crystallizing. The principal feature of supercooled liquids is the strong slowing down of the structural relaxation process resulting from a temperature lowering. This phenomenon is quite huge near the liquid-glass transition temperature T_g, where the cooling causes a freezing of the structural dynamics in a glassy state. The microscopic mechanisms underlying the slowing down of the structural dynamics are nowadays subject of a heated debate in condensed matter physics. In the last years the development of computational and experimental techniques stimulated new theoretical [1–3] and experimental works [4–9] in order to reach a deeper insight on this argument, even if a complete knowledge is far to be achieved because of the complexity of this phenomenon. From an experimental point of view, the main problem is to study the evolution of the dynamics measuring over the entire range from times of the order of picoseconds to 100 s, at which the glass transition conventionally takes place. On the other hand, none of the theories presented till now account for all the features characterizing the dynamics of supercooled liquids. In this scenario, more accurate predictions of the dynamics evolution and effective analytical formula for fitting the data are highly desirable. Moreover, it is important to perform experiments over the extremely wide time range typical of the dynamics of supercooled liquids, as well as to provide more accurate data for a reliable testing of the theoretical predictions. At the state of the art, dielectric spectroscopy, employing quasioptical submillimeter spectrometers besides more conventional frequency response analyzers, is the only technique that can cover the time interval of interest [5]. Alternatively results from different experimental techniques can be combined to cover the widest dynamical range, provided that a careful analysis takes into account the difference among the sensed dynamic observables. However, although the matching of data provided by different techniques is a difficult job, such an approach can greatly enrich the knowledge of the observed relaxation, helping also a stronger definition of the universal behavior of the supercooled state [10,11].

In the middle of the 1980s a new theory, called mode-coupling theory (MCT) [1], was proposed attempting to explain the glass transition phenomenon from a purely dynamical point of view. The MCT originates from the solution of a set of nonlinear equations for the evolution of the correlators of density fluctuations $\langle \rho(t)\rho(0)\rangle$. In its simplest form, called "idealized MCT," the theory predicts a transition at the critical temperature T_c from an ergodic dynamical regime ($T>T_c$), where the correlator of density fluctuation decays to zero, to a nonergodic regime ($T<T_c$), where the correlator remains at a finite value. The theory, even in the ideal version, describes in detail the dynamics of supercooled liquids in the moderately viscous regime where it predicts the existence of two different regions of relaxation (α and β regime) and, as we will see later, accurate functional forms describing the evolution of the time correlator. Despite the theory was formulated for the evolution of density fluctuations taking into account only translational degrees of freedom, in the last years several theoretical [12] and experimental works [4,7,13,14] tested with success the applicability of the theory for density fluctuations involving even the molecular orientational degrees of freedom, as it happens in experiments based on optical Kerr effect.

The optical Kerr effect (OKE) spectroscopy technique measures the evolution of the derivative of the correlation function of dielectric susceptibility related to orientational degrees of freedom. Based on a pump and probe pulsed technique, it allows to measure the relaxation process directly in the time domain, covering a dynamical range from 100 fs to 4 ns with a good signal to noise ratio. These characteristics make OKE spectroscopy particularly important in probing the dynamics of liquids in the hardly supercooled phase and suitable to check directly in the time domain the dynamic evolution scenario predicted by the MCT [13]. Moreover, the

possibility of measuring relaxation times as long as hundreds of picosecond makes possible the comparison with relaxation times measured by dielectric spectroscopy.

The comparison of experimental results obtained by different techniques has been proved suitable for improving the knowledge on relaxation behavior of supercooled systems [5,10,11] but here it is employed using OKE and dielectric measurements on the same compound, the phenyl glycidyl ether (PGE). PGE is an epoxy resin that behaves as a fragile glass forming; the presence of the epoxy group and phenylic rings makes this system particularly suitable for both dielectric and optical study. Moreover, due to the relatively great value of fragility, it presents a huge increase in the relaxation time as the temperature decreases resulting in a good system for testing the glass transition theories.

The present paper is organized in five sections. In Sec. II the MCT model is presented focusing on those elements of interest for our test. Section III is devoted to the description of experimental procedure focusing on the connection between the measured signal and the correlation function of the susceptibilities and also on the description of the experimental apparatus. In Sec. IV we present the analysis and discussion of the results: in the first three parts of the section we present the check of the MCT while in the last part a comparison with dielectric data is proposed. In Sec. V finally some final remarks are added to the discussion.

II. MODE-COUPLING THEORY

Since many reviews and papers about mode-coupling theories [15] are present in literature, here we only recall some results relevant for this work. The ''idealized MCT'' model is based on a number of coupled integro-differential equations that define the evolution of the normalized density fluctuations correlation functions $\Phi(q,t)$. These equations read

$$\frac{\partial^2\Phi(q,t)}{\partial t^2}+\Omega_q^2\Phi(q,t)+\eta_q\frac{\partial\Phi(q,t)}{\partial t}+\Omega_q^2\int_0^t dt' m_q(t-t')\frac{\partial\Phi(q,t')}{\partial t'}=0, \tag{1}$$

where Ω_q^2 is a characteristic frequency of the system, η_q is a friction coefficient due to the contribution of the fast degrees of freedom, and $m_q(t)$ is the memory function that in the hard-sphere model, also called ''microscopic or full MCT,'' is written as a quadratic function of the density correlation functions [16]. The memory function produces the coupling between correlators characterized by different wave vectors q. The full MCT presents the asymptotic solutions that are valid when the temperature is approaching T_c, the critical value. The asymptotic solutions predict some analytical functions that describe the correlators relaxation. These functions apply for all the correlators and the q dependence appears only in the prefactor parameters and it does affect the main relaxation features [16]. Since this work is concerning only with a single wave vector $q\sim 0$, see Sec. III A, we do not report the q dependence in the following MCT predictions.

The asymptotic solutions provide a two-step scenario for the relaxation dynamics: a short time region called β regime, that can be subdivided into the so-called ''critical'' region followed by the ''von Schweidler'' (vS) one, and a long time region called α regime. The MCT β regime, also quoted as β-fast regime, has different nature and features from those of the β relaxation observed in the dielectric spectra, also called β-slow relaxation [5]. In both the vS and α regions the MCT predicts that the density correlators should satisfy the time temperature superposition principle (TTSP).

Hence $\Phi(t)$, for any temperature, is described by a single functional form

$$\Phi_\alpha(t)=f_c\mathcal{F}_\alpha(t/\tau_\alpha), \tag{2}$$

where f_c is the nonergodicity parameter and τ_α is the temperature-dependent time scale that follows this scaling law:

$$\tau_\alpha\propto(T-T_c)^{-\gamma}. \tag{3}$$

In this equation T_c is the ''critical temperature'' of the MCT and γ is a material-dependent parameter. The T_c and γ are key parameters for the analysis of MCT: in fact T_c defines the temperature where the predicted ergodic-nonergodic transition takes place and γ characterizes the relaxation processes present in the glass former.

In the long time part of the α regime the functional $\mathcal{F}_\alpha$ can be reproduced by the stretched-exponential function, also called Kohlrausch-William-Watts (KWW):

$$\Phi_\alpha(t)=f_c\exp[-(t/\tau_\alpha)^\beta], \tag{4}$$

where β is the stretching parameter and τ_α is again the characteristic relaxation time in this region. Both f_c and β are temperature independent, while τ_α scales according to Eq. (3).

The β regime, apart from the shorter time microscopic dynamics, is described by an universal relaxation function:

$$\Phi_\beta(t)=f_c+h|\sigma|^{1/2}g_\lambda(t/\tau_\sigma), \tag{5}$$

where $\sigma=(T_c-T)/T_c$, h is an amplitude factor, and τ_σ is a second characteristic time scale. The $g_\lambda(t/\tau_\sigma)$ is a function dependent only on the parameter λ and is defined by the scaling equation of motion [15,16]. The parameters f_c and h are temperature independent while the characteristic time is described by a second scaling law:

$$\tau_\sigma\propto(T-T_c)^{-1/2a}. \tag{6}$$

The parameters a and λ are material dependent and, as we will show in the following, they are unambiguously and uniquely related with γ. The scaling equation can be solved analytically in the asymptotic limit, $|\sigma|<1$. The leading order solutions are the ''critical decay'' $g_\lambda(t/\tau_\sigma)=(t/\tau_\sigma)^{-1/2a}$ in the very short time region $\Omega^{-1}\ll t<\tau_\sigma$, and the vS decay $g_\lambda(t/\tau_\sigma)=-B(t/\tau_\sigma)^b$ in the following time region $\tau_\sigma<t\ll\tau_\alpha$. The vS decay can be extended up to longer times, t

$\sim\tau_\alpha$, thanks to the next-to-leading order correction [16], hence, for $\tau_\sigma < t < \tau_\alpha$, the density correlator can be described as

$$\Phi_{vs}(t) = f_c - hB(t/\tau_\alpha)^b[1 - K(t/\tau_\alpha)^b]. \quad (7)$$

The b, B, and K parameters are temperature independent. The parameters b, a, γ, and λ can be related through the Euler function Γ by the equations: $\gamma = 1/2a + 1/2b$ and $\lambda = [\Gamma(1+a)]^2/\Gamma(1+2a) = [\Gamma(1+b)]^2/\Gamma(1+2b)$.

An alternative solution of the scaling equation of motion, that applies in the whole β region for $\Omega^{-1} \ll t \ll \tau_\alpha$, can be obtained by a numerical calculation. The calculated $g_\lambda(t)$ and so the relative correlator, see Eq. (5), are called the full β-correlator solutions.

A different route for data interpretation is based on comparison of the measured data with the complete solutions obtained from schematic MCT models [17]. Recently Simionesco and Krauzman [18] proposed a ''two-correlators'' MCT model to fit light-scattering data of some glass formers in order to reproduce properly the spectra in the high frequency region. Indeed, they have been able to fit the spectra features in a very accurate way, including the microscopic and boson peaks features where, vice versa, the ''one-correlator'' schematic MCT model partially failed. Nevertheless some of the approximations used in this model are not safely acceptable. A ''slave-correlator'' MCT model was suggested by Sjögren [19] for the description of tagged-particle motion in a glassy environment, and successfully used by Franosch and co-workers [20] and by Götze [21] to fit measured spectra of some fragile glass formers. The main advantage of these approaches is that they do not rely on the applicability of asymptotic formulas and that all the results on crossover phenomena and preasymptotic corrections are logically included in agreement with the MCT. Furthermore, these theoretical models improve the analysis of the spectra allowing to extend the fitting time and temperature regions, but unfortunately they introduce several substantial numerical and fitting complications. Nevertheless, some authors find that the asymptotic formulas qualitatively give an adequate description of the data [21,22]. In fact, the analysis of light scattering data based on the MCT asymptotic solutions or the two-correlators MCT model give substantially the same value for the MCT parameters, λ and T_c.

The MCT was first formulated for correlation function of the density fluctuations, see Eq. (1), but it should also apply for any observable x that has superposition with density fluctuation, i.e., $\langle \rho(t)x(t')\rangle \neq 0$, [15,16]. Further in the last years several theoretical [12] and experimental works [4,7,13,14] proved with success the applicability of the theory to the molecular orientational degrees of freedom. For this reason it is significant to test the theory with measurements collected by OKE experiment [13].

Finally we would like to stress that MCT predicts a detailed relaxation pattern for the glass-former dynamics with the parameters a, b, γ, and λ that are strongly related and characterized by a defined temperature dependence. So a test of MCT predictions on the experimental results is in our opinion meaningful indeed.

III. EXPERIMENTAL PROCEDURES

A. Time-resolved optical Kerr effect experiment with optical-heterodyne detection

In a transient OKE experiment, an excitation (or pump) polarized laser pulse E_{ex} induces an optical anisotropy in the sample. The relaxation towards the equilibrium of the induced birefringence is probed through the polarization change of a second polarized laser pulse E_{pr} that propagates in the liquid nearly in the same direction of the exciting beam. Increasing the temporal delay between the excitation and the probing pulses allows to measure the relaxation of the induced anisotropy directly in the time domain. In our experiment, the intensity of the depolarized components of the probe beam, which represents the signal field E_s, is revealed through a heterodyne detection scheme. In this configuration E_s interferes on the detector with an extra field, called local field E_{loc}. The E_{loc} is generated by E_{pr} and it is directly proportional to it. The detected intensity is the sum of three contributions: the intensity of E_{loc}, the homodyne contribution, and the heterodyne one. The heterodyne term (HD) is the interesting signal in this experiment and it can be written as [23]

$$S_{HD}(\tau) \propto 2\mathbf{Re}\left(i\eta \int_{-\infty}^{+\infty} dt \left| E_{pr}(t-\tau) \right|^2 \int_{-\infty}^{+\infty} dt' R(t - t') \left| E_{ex}(t') \right|^2 \right), \quad (8)$$

where η is a complex constant that depends on the way E_{loc} is generated (see Sec. III B) and $R(t)$ is the response function of the system.

The response of the system is directly related to the correlation function of the dielectric constant (ε_{xy}) of the liquid [24,25]

$$R(q, t-t') \propto -\frac{\theta(t-t')}{K_B T} \frac{\partial}{\partial t} \langle \varepsilon_{xy}(-q, t') \varepsilon_{xy}(q, t) \rangle, \quad (9)$$

where K_B is the Boltzmann constant, T is the temperature, $\theta(t)$ the Heaviside step function, and q is the wave vector characterizing the spatial modulation of the anisotropy. The induced anisotropy is characterized by a wave vector that is almost zero ($q \sim 0$). When the exciting and probing pulses duration is short (in our experiment 50 fs) compared to the characteristic response time of the system, the heterodyne signal is proportional to the response function of the system $S_{HD}(t) \propto R(t)$. So the HD-OKE technique measures the material response function directly in the time domain and according to the Eq. (9)

$$S_{HD}(t) \propto -\frac{1}{T} \frac{\partial}{\partial t} \Phi_{\varepsilon\varepsilon}(t), \quad (10)$$

where $\Phi_{\varepsilon\varepsilon}$ is the correlation function of dielectric constant.

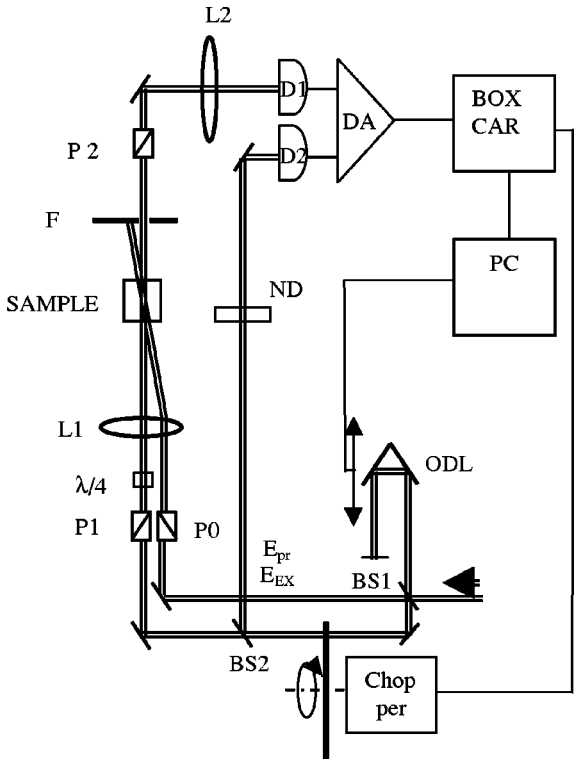

FIG. 1. Experimental setup used for OKE measurement. BS1 and BS2, beam splitters; $P0$, $P1$, and $P2$, Glann-laser polarizers; $L1$ and $L2$, quartz lenses; F, optical cleavage; ND, variable neutral density filter; DA, differential amplifier; ODL, optical delay line.

B. Laser system and optical setup

The laser system used for the HD-OKE experiment is composed of a Kerr lens mode-locked Ti:Sapphire oscillator and a chirped pulse amplification system [26]. The amplification system is a regenerative Ti:Sapphire cavity pumped by a Nd-YLF (yttrium lithium fluoride) laser, it delivers 500 μJ, 50-fs pulses at a repetition rate of 1 kHz. In the experimental setup, see Fig. 1, the laser beam is divided into the exciting and the probing beam (about 80%-20%) by a beam splitter BS1. The exciting beam arrives directly on the sample passing through a polarizer $P0$; the probing beam goes through an optical delay line controlled by a computer, then it is splitted (BS2) generating the so-called reference beam and finally it arrives to the sample through a polarizer $P1$ that selects the direction of polarization (45° respect to the pump beam). Both the E_{ex} and E_{pr} are directed on the sample by a 600-mm focal length lens $L1$ that realizes the spatial superposition of the two pulses. A polarizer $P2$ crossed respect to $P1$ is placed after the sample; a wide band $\lambda/4$ plate is placed between $P1$ and the sample and adjusted for minimum leakage of the $P2$ polarizer in presence of the sample and of $L1$. E_{loc} used for the heterodyne detection is generated by a small rotation of the $\lambda/4$ plate (in our experiment the rotation is of an angle $\varepsilon \sim 3°$) and it is proportional to the probe field: $E_{loc} = \eta E_{pr}$. In this configuration the η constant that appears in the heterodyne term, see Eq. (8), is $\eta = \varepsilon + i\varepsilon$ [23]. Actually this experimental procedure produces both a birefringent and a dichroic contribution. Indeed the dichroic signal is very small and it can be safely neglected [27].

The signal, so generated, contains three terms: a constant intensity produced by E_{loc}, a homodyne S_{HO}, and a heterodyne term S_{HD}. To eliminate the first constant term the signal is revealed through a differential photodiodes system: one diode $D1$ measures the whole signal coming from the sample; the other diode $D2$ is balanced with the reference beam to compensate the E_{loc} intensity. The output of the differential is set to zero, in absence of the pump beam, by means of a continuously variable neutral density filter placed in front of $D2$ diode. A boxcar gated integrator, synchronized to a mechanical chopper placed on the exciting beam, collects the output of the differential diode amplifier allowing an automatic subtraction of the other backgrounds present in the signal. The homodyne contribution is eliminated by subtracting two different measurements taken with opposite direction of the rotation of the $\lambda/4$ plate. In fact, these two measurements are characterized by positive terms for S_{HO} and by the S_{HD} signal with opposite signs. A set of calibrated neutral density filters were used in order to increase the dynamic range of the apparatus.

C. Data collection

The HD-OKE data are composed by a number of time points corresponding to the scan of the optical delay line. The present data have from 1800 (high) to 2500 (low-temperature data) time-points. For each time point the signal intensity is the average over 500 laser pulses. The wide experimental time window is collected with three different scans composed of time points spaced in different way: from 0 ps to 4 ps we use a time step of 5 fs, from 2 ps to 18 ps we use a time-step of 10 fs, and for the remaining time window a logarithmic time step. The scans are matched to rebuild a single data, using an extreme attention to the signal consistency in the overlapping time regions. We used laser pulses of different energy and temporal length to optimize the signal intensity: pump pulses of 50 fs and 1.2 μJ (transform limited) are employed in the short scan and pump pulses of 1 ps and 12 μJ (chirped) in the long scan. With longer laser pulses it is possible to transfer a larger quantity of energy to the system without increase the instantaneous intensity of the pulse. The signal is then characterized by a better signal-noise ratio that allows to reach longer temporal region, as we can see in Fig. 2. Using the heterodyne detection and stretched pulses more than five intensity decades and more than six temporal decades signals are detected.

PGE sample (Fig. 3), provided from Aldrich with a purity greater than 99%, was used without further purifying. The sample was placed in a 2-mm-thick quartz cell of very good optical quality. The temperature was controlled by a cryostat system within ± 0.1 K.

The HD-OKE data on PGE sample are collected in the temperature interval 265.3 K–352.5 K. In Fig. 3 we report all the experimental data normalized to the instantaneous electronic response peak.

IV. ANALYSIS AND DISCUSSION

OKE measurements show clearly three different temporal regions (Fig. 3): the first one ($\sim 0-200$ fs) is characterized

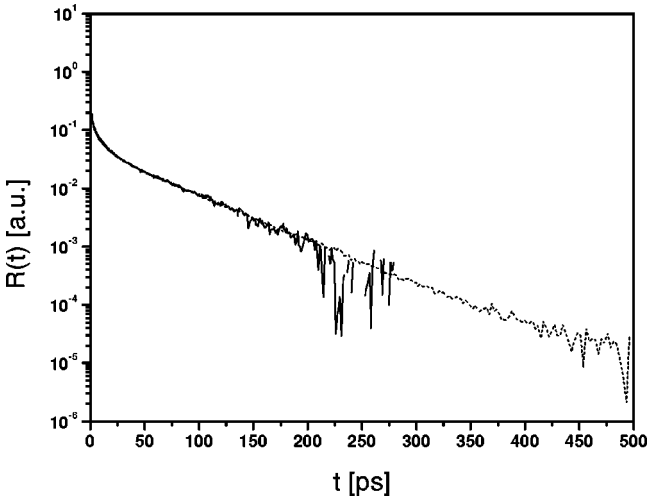

FIG. 2. Heterodyne detected OKE signals (R in arbitrary unit) of PGE at 322.9 K represented in a semilogarithmic plot. The continuous line represents a measurement performed with 50-fs pulses, the dotted line is the measurement with 1-ps pulses.

by an instantaneous response that has to be mainly addressed to the electronic dynamics, the second one (from ~ 200 fs to about 100 ps depending on temperature) where the response is weakly dependent on temperature, and the third region where the signal exhibits a slow relaxation strongly dependent on temperature. In the first picoseconds, OKE measurements show the presence of the oscillatory dynamics due to intramolecular vibrational degrees of freedom, corresponding to Raman frequencies: $\upsilon \cong 245$ cm^{-1} and 332 cm^{-1}. As we have seen in Sec. II, the MCT predictions concern the correlation function behavior, while OKE measurements is proportional to the system response function, i.e., to the time derivative of the correlation function of the dielectric constant [Eq. 10]. So, in order to check the MCT predictions, the OKE data have to be compared with the derivative of the

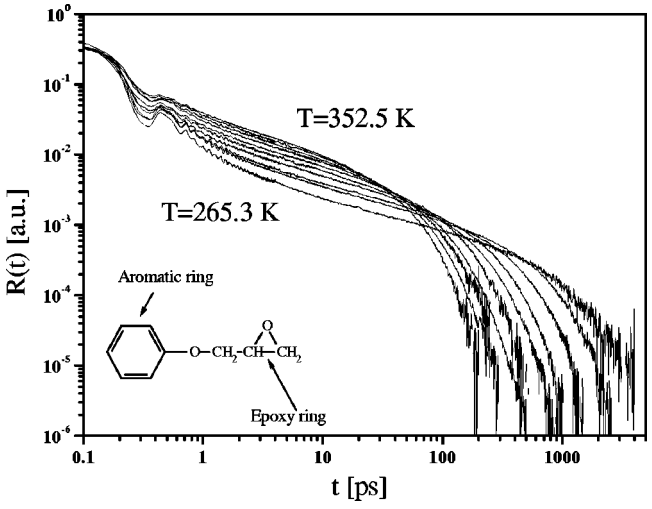

FIG. 3. Bilogarithmic plot of OKE signals vs time t of PGE for the temperatures: 265.3, 273.8, 283.5, 293.1, 303.4, 312.9, 322.9, 333.4, 343.0, and 352.5 K.

MCT functional. In the β region the response function must be reproduced by the time derivative of Eq. (5), that is,

$$R_\beta(t) = -\frac{\chi_\sigma}{T}\frac{\partial g_\lambda(t/\tau_\sigma)}{\partial(t/\tau_\sigma)}, \tag{11}$$

where $\chi_\sigma = h|\sigma|^{1/2}\tau_\sigma^{-1} \propto (T-T_c)^{(a+1)/2a}$. In the α region $R(t)$ should be the time derivative of Eq. (2):

$$R_\alpha(t) = -\frac{\chi_\alpha}{T}\frac{\partial}{\partial(t/\tau_\alpha)}\mathcal{F}_\alpha(t/\tau_\alpha), \tag{12}$$

where $\chi_\alpha \propto f_c\tau_\alpha^{-1} \propto (T-T_c)^\gamma$. Also in the last part of the α regime the MCT theory predicts an analytical form of the correlator, the KWW law [Eq. 4], so the response function becomes

$$R_\alpha(t) \propto f_c\left(\frac{\beta}{\tau_\alpha}\right)\left(\frac{t}{\tau_\alpha}\right)^{\beta-1}\exp[-(t/\tau_\alpha)^\beta]. \tag{13}$$

In the vS time region the MCT predicts vS law [Eq. (7)] that gives the following response function:

$$R_{vs}(t) \propto B_1 t^{b-1} + B_2 t^{2b-1}, \tag{14}$$

where $B_1 = hBb/\tau_\alpha^b$ and $B_2 = -2hBKb/\tau_\alpha^{2b}$ with reference to notation of Eq. (7).

One difficulty of testing the MCT predictions is to establish the temporal range of validity of the α and β regime. To overcome this difficulty we used the following procedure. First we tested the existence of a temporal region in agreement with the TTSP: in doing this we have superimposed the final part of each curve by scaling them by an amplitude and a temporal factor. In this way it was possible to find the values of the amplitude factor χ_α and of the scaling time τ_α. Within the region of validity of the TTSP we fitted each experimental curve to $R_\alpha(t)$ [Eq. (13)]. The temporal window has been selected to optimize the fit quality and the best values of the parameters were found through a least square fitting based on a Levenberg-Marquardt method. To reproduce the experimental curve in the faster temporal region, limited at long times by the validity of the KWW law, we tested the validity of the vS law with the next-to-leading-order correction [Eq. (14)]. As before, the fit time interval was chosen to optimize the fit quality. From vS fit it has been possible to obtain the values of the amplitude parameters B_1 and B_2 and of the exponent b that is connected to exponential parameter λ.

The analysis of the first picoseconds OKE measurements is troubled by presence of intramolecular oscillations that prevents a safe and independent test of the critical decay in this time region. In order to extend signal analysis to the fast time region we used the MCT full β correlator, Eq. (5). Using a calculus program we produce a numerical curve equivalent to the derivative of $[\Phi_\beta(t) - f_c] = +h'|\sigma|^{1/2}g_\lambda(t')$. The program, for any value of the input parameters (λ and T_c), gives numerical curve where the time t' and amplitude h' scale are in arbitrary units and they have to be normalized to the experimental scales. So comparing

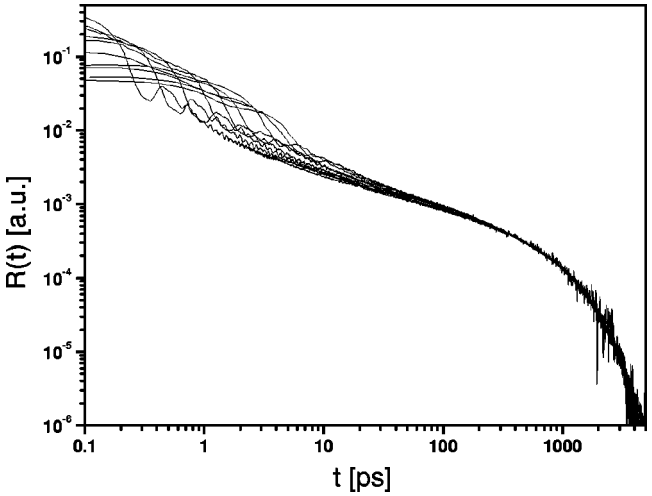

FIG. 4. Bilogarithmic plot representing the master plot of OKE data obtained by scaling the time and amplitude of each signals. All the signals are superimposed, in the long time region, taking as reference the measurement at 265.3 K.

the full β-correlator curves to the OKE data we found the parameters χ_σ and τ_σ for each temperature and hence from their scaling law the value of λ and T_c. Finally we compared the values of λ and T_c found from the different analysis (α regime, vS regime, and full β correlator).

A. Master plot and time temperature superposition principle

The first objective of the analysis was to check the TTSP and to define the temporal region where it applies. We have rescaled all the OKE signals, corresponding to different temperatures, in time and amplitude on 265.3 K signal, which is the lowest measured temperature. As we can see in Fig. 4 all the signals rescale onto a master curve. The time scaling factors have been subsequently multiplied by τ_α obtained from the KWW fit of the 265.3 K curve in order to get the real values of the α-relaxation times. The scaling procedure allows to get the amplitude χ_α and the time τ_α scales of the α regime, see Eq. (12), and it turns out to be a precise procedure thanks to the signal-noise ratio. From χ_α and τ_α we can calculate the value of a parameter proportional to f_c; in fact from Eq. (12) $f_c \propto \chi_\alpha \tau_\alpha T$. Errors affecting τ_α were computed propagating the error of the corresponding scaling temporal factor with that of the value of τ_α of the curve at 265.3 K, while that of f_c is computed from the errors of the two scaling factors.

The values of the relaxation time τ_α are presented in Fig. 5(b) in a linearized plot with the relative fit according to Eq. 3. The theoretical curve well reproduces experimental data by yielding $T_c = (229 \pm 3)$ K and $\gamma = 2.6 \pm 0.2$ corresponding to $\lambda = 0.76 \pm 0.04$. Also in some other molecular glass formers it was found that the MCT describes the temperature dependence of τ_α in the moderately viscous regime at high temperature [7,5,13].

In Fig. 5(a) the calculated values of f_c are presented. Though they are scattered they do not present a real trend and assuming, as expected from the theory, a constant value

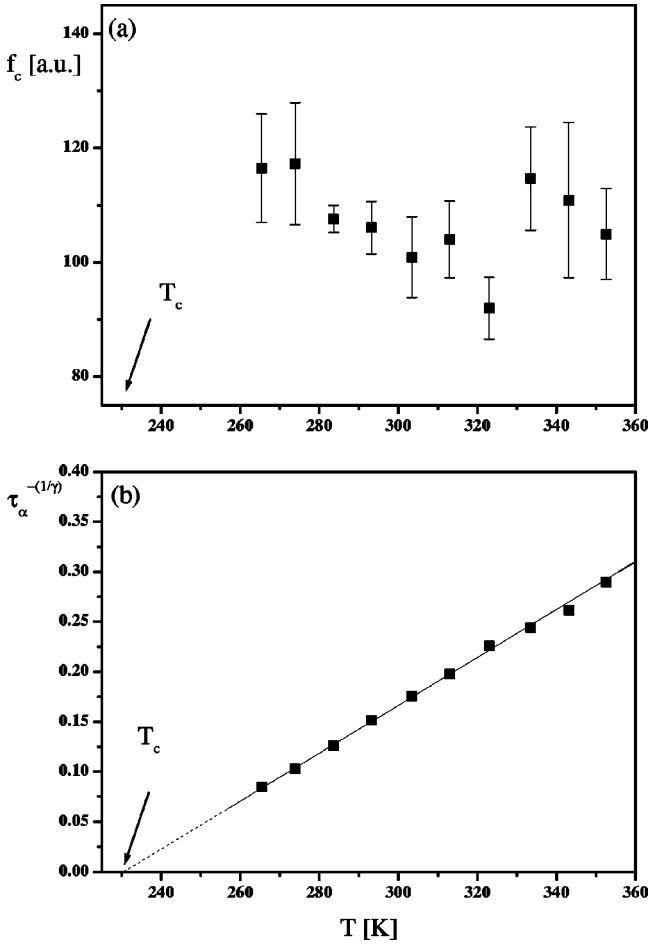

FIG. 5. (a) Plot of the nonergodicity factor f_c (squares) vs temperature T obtained from the time temperature superposition principle. (b) Plot of τ_α (squares) vs temperature T as deduced from the scaling procedure (see text). The continuous line represents the linear fit according to the scaling law Eq. (3) while the dashed one is its extrapolation down to T_c. The errors are not reported because they are smaller than the symbols.

it is possible to calculate its mean value: $f_c = 106 \pm 11$ (one standard deviation is taken as error). In a previous analysis of OKE measurements of *m* toluidine [13] it was found that f_c becomes larger as temperature decreases. Deviation from the prediction of the MCT was found in the analysis of dielectric data and polarized Brillouin light scattering on propylene carbonate but the same authors move some doubts about their evaluation of f_c [21,28]. However, in recent analysis of polarized Brillouin light-scattering analysis of *m* toluidine and toluene a temperature-independent value of f_c was found for $T > T_c$ [22,29].

B. Slow dynamics and the MCT α regime

The second step of the analysis was testing the KWW on the long time relaxation region. The derivative of the KWW law [Eq. (13)] well reproduces the experimental curves in the long times region as we can see in Fig. 6 where four of them are represented with respective fit in a log-log plot. It is important to note that this fitting procedure is independent

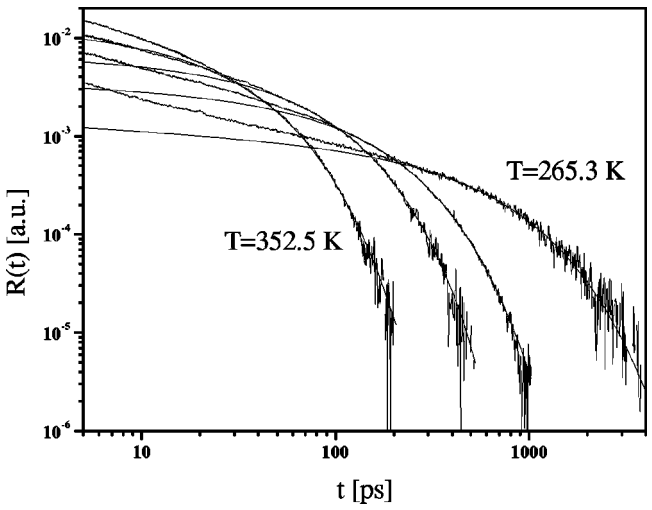

FIG. 6. Plot of the long time region of the OKE signals with the corresponding fit with the KWW law. From top to bottom the curves correspond to 352.5, 312.9, 393.1, and 265.3 K.

from the verification of the TTSP and then it is a second independent test of the α regime of the MCT. Thanks to the good signal-noise ratio it was possible to extract the values of f_c, τ_α, and β for each temperature. In Table I we present the values of τ_α and f_c as obtained from the fit and from the scaling procedure of the master plot and also the values of β from the fit.

As we can see from Table I the parameter β does not present any temperature dependence: in fact, though the spread is wide, all the values, except that at 333.4 K, are consistent with each other in the error bar. The mean value of this set of data results $\beta = 0.91$. The temperature independence of β is in agreement with the MCT and it is a necessary condition to the α-relaxation process to obey the TTSP. Also in the previous OKE study on *m* toluidine [13] and light-scattering studies of toluene and propylene carbonate a constant value of β was found [28,22]. However, in other cases analysis of dielectric or light-scattering measurements performed in the frequency domain reveals an increase of β with T [5,29,30] with a tendency to almost saturate at a certain value at high temperature. Finally it is noteworthy to note that recently some photocorrelation measurements on PGE were published corresponding to a temperature range below 211 K, i.e., below T_c [31]. Even at this low temperature the long time region of the relaxation process can be fitted to a stretched exponential law with a constant but lower value of the parameter β. The difference in the β value obtained from OKE and photocorrelation measurements can be ascribed to the different experimental techniques used or to the two different temperature interval investigated, which could be separated by a temperature region characterized by a decreasing of β. Some further studying would be necessary to choose between these two possibilities.

TABLE I. Values of the parameters related to the MCT α regime as from the fit with the derivative of the KWW (last three columns) and from the master plot scaling procedure (second and third columns).

T (K)	f_c (a.u.)	τ_α (ps)	f_c (a.u.)	τ_α (ps)	β
265.3	116±9	610±41	125±8	588±25	0.88±0.04
273.8	117±7	371±34	120±5	373±11	0.93±0.03
283.5	108±2	218±7	113±3	218±7	0.92±0.02
293.1	106±5	135±9	108±3	136±4	0.92±0.01
303.4	101±7	92±7	103±3	96±3	0.90±0.02
312.9	104±7	68±4	110±3	69±2	0.93±0.03
322.9	81±5	48±4	84±3	50±2	0.93±0.02
333.4	115±9	39±3	117±7	38±2	0.87±0.02
343.0	111±14	33±4	117±3	32±2	0.90±0.02
352.5	105±8	25±2	102±7	27±2	0.93±0.03

The values of f_c are presented in Fig. 7(a): it is peculiar to note that nearly the same spread is present in the set of values of f_c obtained both from the master plot [Fig. 5(a)] and the fit. This evidence seems to reveal a slight dependence of the parameter from the temperature. However the accuracy of the values does not allow to confirm this hypothesis. In fact, while the values at lower temperatures seems to present a linear increase we must note that the increasing over the whole temperature range is only of 6.8% that is of the same order of the error of the value at higher temperatures. We can conclude that according to the experimental uncertainty f_c presents no temperature dependence in this region as predicted from the theory. The mean value obtained from the fit is $f_c = 110 \pm 12$ and it is consistent with that obtained from the master plot.

Finally the characteristic times τ_α obtained from the fit give a second test of the scaling law provided for by the MCT. As we can see in the Table I these values of the relaxation time are very similar to those obtained from the master plot scaling procedure as expected from the theory. Only the values at 265.3 K disagree in a more pronounced way though they are consistent in the error bar. However, we must note that the measurement at this temperature is on the limits of the time window of the experiment and this fact results in a less good evaluation of the time τ_α as evident from the great error assigned to it. Values of $\tau_\alpha(T)$ from the KWW function were fitted to Eq. 3 that led to $T_c = (227 \pm 5)$ K and $\gamma = 2.7 \pm 0.2$ corresponding to $\lambda = 0.78 \pm 0.04$ [Fig. 7(b)]. All these values of the parameters are completely consistent with those found by the master plot. This is an important proof of consistency because though the master plot gives less precise values of τ_α, it is a fitting independent and simple method of obtaining τ_α.

C. Fast dynamics and the MCT β regime

In the intermediate time region we fitted the signal to the vS law with the next-to-leading-order correction [Eq. (14)]. In Fig. 8 four measurements with related fitting curves are represented; we can note that the vS law reproduces a temporal region that increases with decreasing temperature. From a least square fitting procedure we extracted the values of the parameters. The parameter *b* presents a set of values scattered around the mean value $b = 0.59 \pm 0.03$ that corre-

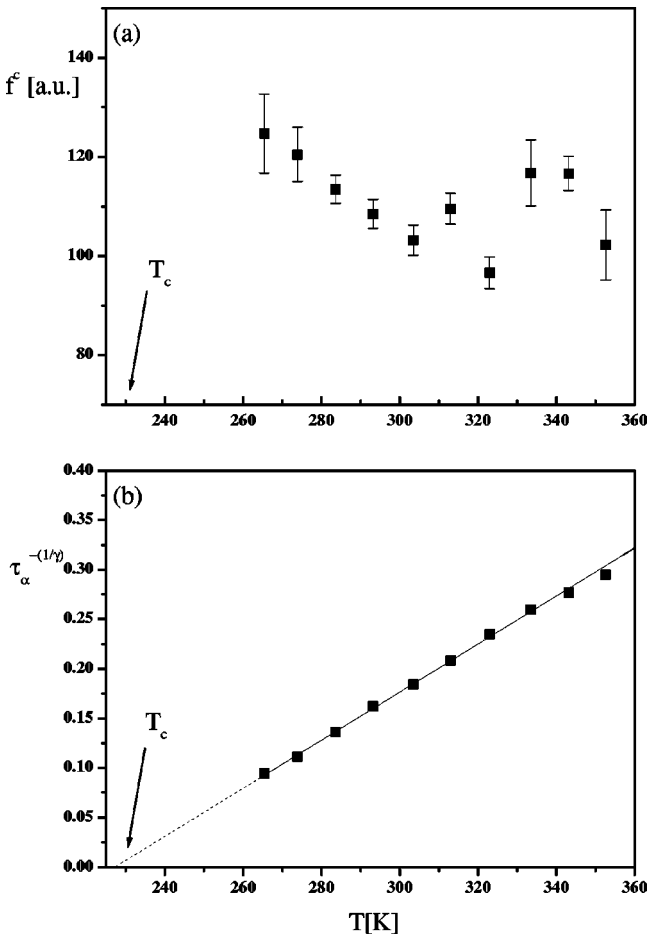

FIG. 7. (a) Plot of the nonergodicity factor f_c (squares) vs temperature T. The values of f_c are obtained from the fitting procedure employed with the derivative of the KWW law. (b) Linearized plot of τ_α (squares) vs temperature T with the correspondent fit according to the scaling law, Eq. (3). The dashed line represents the extrapolation of the fit down to T_c. The errors are not reported because they are smaller than the symbols.

sponds to $\lambda = 0.73 \pm 0.02$. This value is in good agreement with that obtained from the α-regime analysis. Moreover, from the amplitude parameters B_1 and B_2 we can extract the values of the second-order correction parameter K, in fact $K = 2B_2/B_1\tau_\alpha^b$ [Eq. (14)]. In this calculation we have used the values of τ_α obtained from the fit with the KWW law and b from the previous analysis. This procedure gives values of K affected by a great error but at the moment this is the only experimental method to obtain the K parameter. We find, in the experimental uncertainty, no temperature dependence for the K parameter [Fig. 9] as predicted from MCT theory. The mean value from this analysis is $K = 0.27 \pm 0.03$ that is in agreement with the value of the same parameter as from a previous work on the *m*-toluidine [13].

Finally a deeper analysis of the fast time region has been performed using the MCT full β correlator. We used a calculus program to produce numerical curves equivalent to the time derivative of the β correlator. For each couple of λ and T_c parameters the program produces a family of numerical curves each of them defined by the experimental temperature

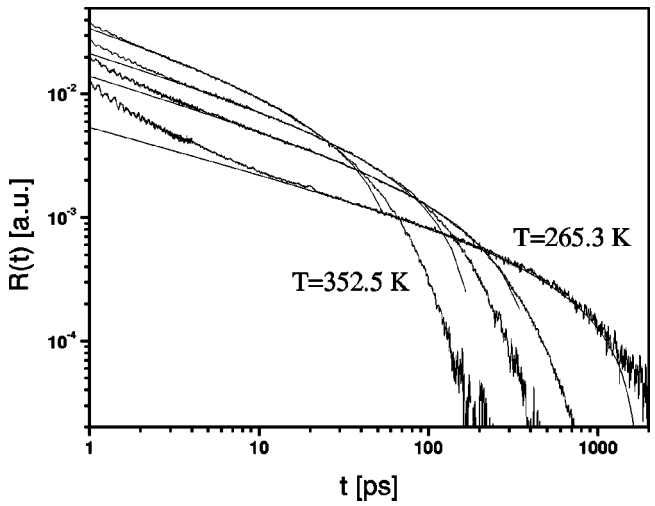

FIG. 8. Plot of the intermediate region of the OKE signal for the temperature 352.5, 312.9, 293.1, and 265.3 K with the correspondent fit according the vS law.

T. These curves should reproduce the experimental data apart from an amplitude and a temporal factor independent of the temperature. With the OKE data this was only partly possible: indeed we found a single temporal factor, valid for all temperatures, but the amplitude factor has to be varied for each temperature. Finally we have chosen the full β-correlator curves corresponding to an unique value of λ and T_c, that are able to reproduce the largest number of experimental data in the widest temporal range. From this analysis we found that according to our judgement $\lambda = 0.73$ and $T_c = 230$ K give the best fit. However, curves relatives to $\lambda = 0.76$ and $T_c = 230$ K and $\lambda = 0.69$ and $T_c = 233$ K also fit the experimental data but in a shorter temporal region. Since this analysis is not based on a least square fitting procedure it is not easy to choose the best values for the parameters, nevertheless we estimated a 5.4% error for the exponential parameter ($\lambda = 0.73 \pm 0.04$) and a 1.3% error for the critical temperature ($T_c = 230 \pm 3K$). As we can see in

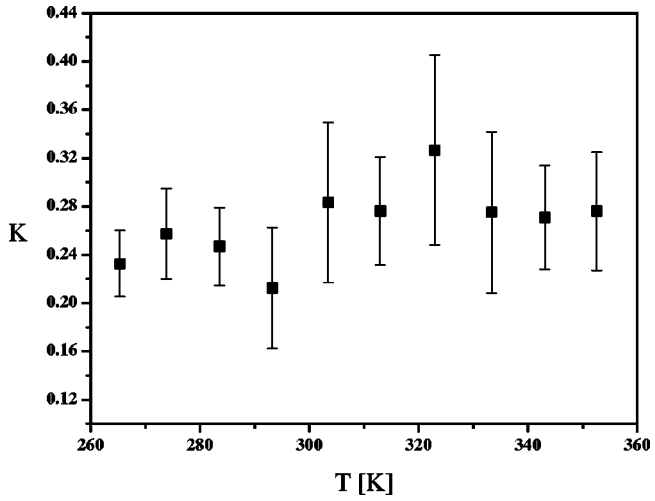

FIG. 9. Values of the amplitude parameter K of the next-to-leading-order correction of the vS law [see Eq. (7)].

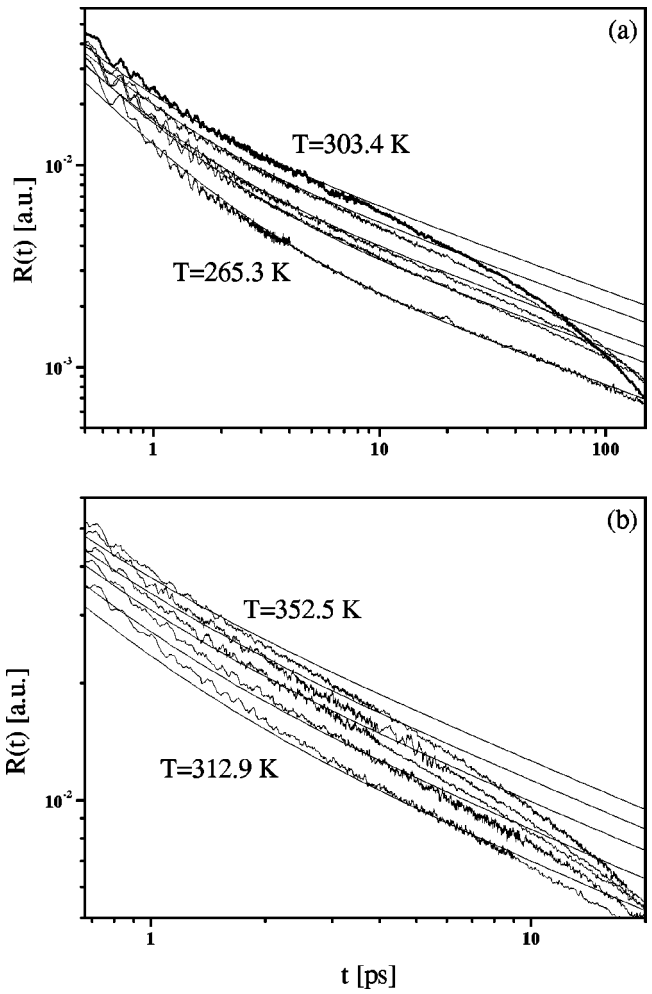

FIG. 10. Bilogarithmic plot of the short time region of OKE signals with the fit according to the derivative of the full β-correlator function (continuous line) for temperature from 265.3 to 303.4 K [panel (a)] and for temperature from 312.9 to 352.5 K [panel (b)]. In panel (a) we can note a good superposition between experimental and theoretical curves, while for the curves in panel (b) the agreement is less reasonable.

Fig. 10(a) the fit with the full β correlator is fairly good in the temperature range from 265.3 K to 303.4 K while the accordance is less reasonable on the upper temperatures particularly for $T>322.9$ K [Fig. 10(b)]. On the other hand the MCT predicts the full β correlator as a law effective in a temperature region near T_c while these last three curves correspond to measurements at temperature more than 100 K higher than the critical temperature $[|(T_c-T)/T_c|>0.45]$. So it does not surprise if the predictions of the theory are not verified for the high-temperature range. Furthermore, we note that the full β correlator superimpose to the vS law only in the measurements corresponding to lower temperatures ($T<293.1$ K). The values found for λ and T_c are in very good agreement with those obtained from the analysis of the long time (α region) and intermediate time (vS region) regions. As we already explained the scaling procedure of the full β correlator needed one temporal rescaling factor only but different amplitude factors. However, calculating the new

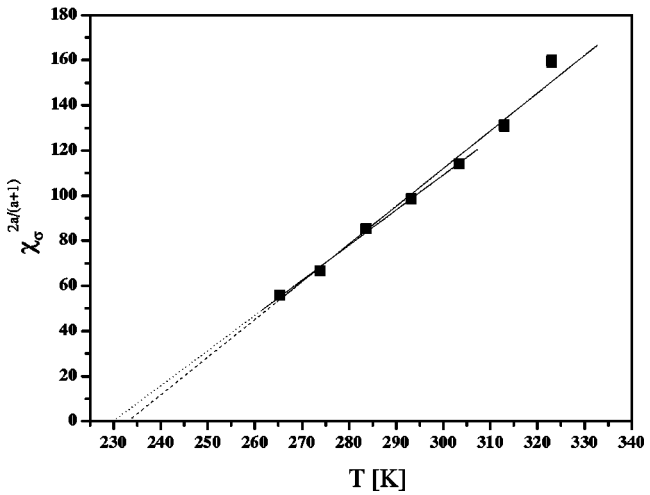

FIG. 11. Values of the amplitude parameter χ_σ vs temperature T as obtained from the fit with the full β correlator (see text). The values are represented in a linearized plot. Only the values for $T<322.9$ K are shown. Two fits are presented (straight lines): the first one is over the whole temperature range ($T_c=233$ K) while the second one is performed on data for $T<303.4$ K ($T_c=230$ K). The dashed and the dotted lines represent the extrapolation of the curve fit down to T_c.

amplitudes χ_σ of the β correlator for each measurement with temperature $T<322.9$ K, we can still represent them in a linearized plot, $\chi_\sigma^{2a/(a+1)}$ vs T [Fig. 11], by using the value $a=0.31$ corresponding to $\lambda=0.73$. The best value of T_c that allows to reproduce by a linear fit is $T_c=233$ K [continuous line in Fig. 11], which is greater than those found in the previous analysis. Indeed, as we showed, the full β correlator is not able to reproduce properly the experimental curves for $T>303.4$ K and so we tried to fit only the values of $\chi_\sigma^{2a/(a+1)}$ up to this temperature. The new linear fit gives $T_c=230$ K [dashed line in Fig. 11], which is in reasonable agreement with that found from the analysis of the α region. The agreement of the various values of λ found from the analysis of the different temporal regions proves the reliability of the connection between the parameters characterizing the long time region γ and the vS region b and their dependence from the unique parameter λ.

D. Comparison between results obtained by OKE and by dielectric spectroscopy

Comparison between experimental results obtained by different spectroscopic techniques can improve the understanding of glass-former dynamics. Several studies already exist on this subject but, unlike its importance, the general scenario is still unclear. The difficulty of this kind of analysis originates both from considering data that often coverdifferent spectral ranges and from the fact that the dynamics of the system is investigated by different probes. The present study, to the best of our knowledge, is the first attempt of performing such a comparison between OKE and dielectric measurements. There are two main difficulties in the present comparison: the data are collected in different domains (frequency and time); both techniques measure collective re-

orientation times but these are related to different correlation functions characterized by different orders of the Legendre polynomials. Nevertheless a comparison between the characteristic time scales, obtained by these two techniques, could indicate the consistency of the relaxation processes.

Dielectric measurements on PGE were carried out using the frequency domain reflectometry technique. The measurements were carried out on the frequency interval between 100 kHz and 30 GHz at temperatures between 353.1 K and 245.6 K. We employed two different experimental apparatuses: the network analyzer HP8753ES with $C_0 \cong 3.5$ pF was employed in the frequency ranges 5×10^4 Hz–1.8×10^9 Hz and the network analyzer HP8722D with $C_0 \cong 0.15$ pF in the range 5×10^7 Hz–4×10^{10} Hz. More details about experimental apparatuses are elsewhere reported [32]. In the investigated temperature range, the spectra of the dielectric constant ε clearly show the presence of the structural relaxation α which shifts towards lower frequencies as temperature decreases, according to the behavior of the optical measurements. Indeed, our dielectric spectral range, even covering more than 6 decades, does not allow to reach the high frequency region that corresponds to the β region predicted by the MCT. The experimental curves were fitted to the phenomenological Cole Davidson function [33] $\varepsilon(\omega) - \varepsilon_\infty = \Delta\varepsilon/[1+(i\omega\tau_\alpha^{cd})^{\beta_{cd}}]$, where ε_∞ is the high frequency limit of $\varepsilon(\omega)$, β_{cd} is a shape parameter, $\Delta\varepsilon$ is the relaxation strength, and τ_α^{cd} is the characteristic time of the relaxation. The complete analysis of the dielectric parameters is beyond the aim of the present paper and will be presented in a forthcoming paper.

In order to connect the dielectric and OKE results we transformed the dielectric relaxation time τ_α^{cd}, measured in the frequency domain, into the corresponding decay time τ_α of the KWW function using an appropriate numerical relation [34]. By comparing the transformed dielectric relaxation times with OKE ones, we found the former to be appreciably shorter than the latter [Fig. 12(a)]. Nevertheless the temperature dependence of the two parameters is almost the same, which would confirm that the two techniques detect the same structural process. In fact, we get a good superposition of the two time scales rescaling the OKE relaxation times by a temperature independent factor, $\Xi = 0.58$. This superposition applies in the whole temperature range where data from both the techniques are available [Fig. 12(b)].

The Debye rotational diffusion model makes precise predictions about the dynamical properties of a symmetric-top molecule diffusing through a Brownian rotational motion [35]. In particular it predicts that the rotational correlation function relaxes exponentially with a relaxation time defined by the order of the Legendre polynomial. According to strong approximations, the dielectric response can be connected with the first-order Legendre polynomial and the OKE to the second-order Legendre polynomial. Following the Debye model we should find $\tau_{diel}/\tau_{oke} = 3$, but this prediction is not supported by our experiments since we find $\tau_{diel}/\tau_{oke} = 0.58$. A different model for the rotational dynamics of a symmetric-top molecule has been made by Ivanov [36], describing the process as a continuous jump process.

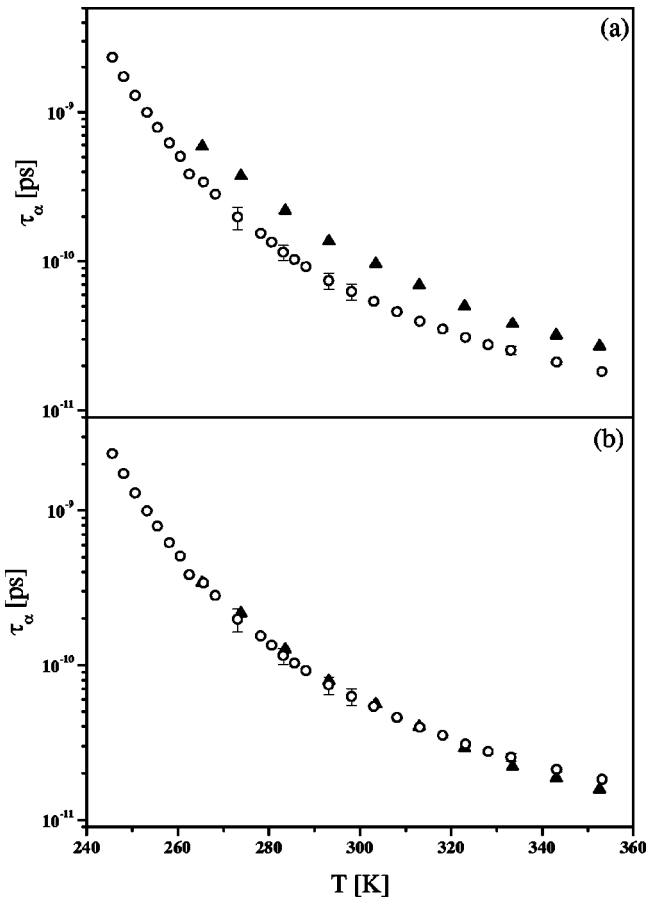

FIG. 12. (a) Plot of OKE (up triangle) and dielectric (open circle) τ_α vs temperature *T*. We note that the former are larger than the latter. (b) Plot of rescaled values of the τ_{oke} (up triangle) and values of the dielectric time (open circle). We can note that the two time scales superimpose by scaling for a constant factor (0.58).

According to this theoretical model the ratio of the two time scales should be $\tau_{diel}/\tau_{oke} = 1$. So again our experiment does not support the model. However these disagreements do not surprise, since the approximations used in these theoretical models are indeed too strong.

Furthermore, our findings about the comparison between dielectric and optical characteristic time scales qualitatively agree with previous light-scattering and dielectric experiments on polystyrene and diglycidyl ether of bisphenol-*A* (DGEBA) [11,37]. Comez *et al.* [11] proposed to single out the cause of such behavior in the different microscopic probe that allows the determination of the dielectric and of the optical measurements, namely, for DGEBA (and also for PGE), the epoxy ring and the aromatic ring, respectively. In particular, they suggested that the different sizes of such molecular subunits cancorrespond to a difference of the effective hydrodynamic volume V_h, which enters in the Debye-Stokes-Einstein (DSE) equation,

$$\tau = V_h \eta / kT,$$

where η is the shear viscosity of the system. Consequently, one obtains different relaxation times for the response func-

tion of the two observables [11]. In particular, for light-scattering and dielectric relaxation time of DGEBA they found an almost constant factor $\Xi = 0.13$ between the two time scales in a restricted temperature range extending above $T_c \simeq 1.2\ T_g$. The authors speculated that approaching T_g the hydrodynamic volume characteristic of the dipolar orientation remains constant, which was supported by the validity of the DSE equation for DGEBA, in a temperature interval of more than 100 K. On the contrary, the optical effective volume could decrease with decreasing temperature, determining the approach of the dielectric and optical characteristic time scales observed for DGEBA for temperature $T < 1.2 T_g$. This fact cannot be verified on PGE, due to the less broad temperature interval where the OKE time scale have been measured.

V. SUMMARY AND FINAL REMARKS

In this paper we have presented measurements of the birefringence relaxation carried out by OKE experiment and a test of the idealized MCT. We have also compared the characteristic times of the α-relaxation process present in OKE measurements with those of the structural process of dielectric spectra. The use of picosecond pulses and of the heterodyne detection system in the OKE experiment allowed measuring the relaxation processes over a large temporal window till 4 ns with a good signal-noise ratio. So it has been possible to test the MCT in a wide temperature interval covering the liquid and supercooled region.

As we have seen in Sec. IV OKE signal presents three temporal region. We showed that the functional forms predicted by the idealized MCT (full β correlator, vS next-to-leading-order corrected and KWW laws) reproduce the signal in the whole time region, from about 1 ps, almost for all the temperatures investigated. Only the microscopic dynamics due to electronic response of the system and to the excitation of internal degrees of freedom cannot be reproduced since the idealized MCT does not include such degrees of freedom. As an example of the ability of the theory to reproduce experimental data, in Fig. 13 we show the OKE signal at 273.8 K and the corresponding fitting curves. From the data analysis we obtained, for each temperature, the values of the parameters characterizing the relaxation processes. In particular, from the TTSP and from the KWW fits we obtained agreeing values of τ_α and f_c, whose temperature dependence is well predicted by the MCT. Moreover the stretching parameter β does not depend on temperature as it is provided by the theory and as it is required for the validity of the TTSP. The vS fit gives us values of b and of the amplitude parameter K independent from temperature as it is stated from MCT. It is noteworthy that until now this is the second experimental measurement of K parameter and the two available K values, corresponding to different glass formers, are substantially identical. These preliminary results suggest a very slight dependence of K from the molecular properties of the glass former. Finally we also noted that β-correlator solution applies in a shorter temperature range than the TTSP. We performed the data analysis using different checks of the MCT: the TTSP and the KWW law in the long times relaxation region, the full β correlator in the fast times region. So we extracted in three independent ways the characteristic parameters of the MCT theory: λ and T_c. Their values are reported in Table II: they are in very good agreement. This is indeed a severe check of consistence for MCT that has been completely passed in the present work.

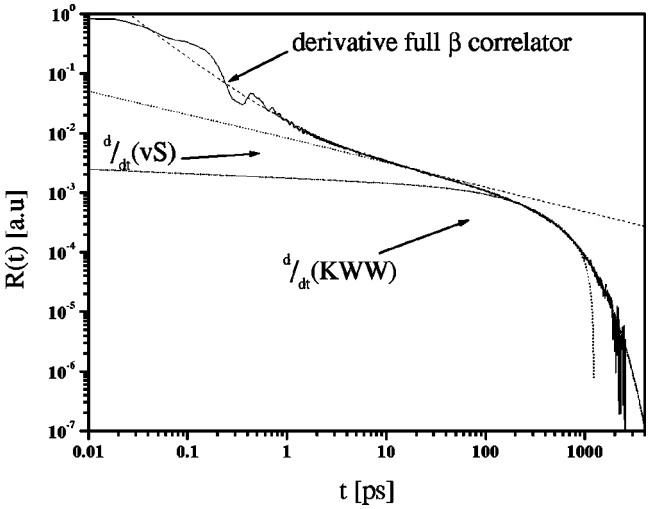

FIG. 13. Bilogarithmic plot of the OKE signal at 273.8 K vs time t and of the corresponding fit according to MCT laws: the derivative of the full β correlator (dashed line), the derivative of vS law (dotted line), and the derivative of the KWW law (dashed-dotted line).

Here a comparison of structural relaxation measured by OKE and dielectric spectroscopy is presented. In a wide temperature region, above T_c, we found the structural relaxation times τ_α of optical processes larger than the dielectric ones. Nevertheless the temperature dependence of these two set of relaxation times is substantially identical, in fact it is possible to superimpose them by a temperature-independent factor. These results suggest the presence of a unique slowing-down effects that shows up on different time scales, depending on the observable probed. So concerning the slow dynamics, the present work is confirming a universal aspect of the structural relaxation properties. Undoubtedly, the comparison between results obtained by different experimental techniques is a very interesting topic that only recently started to be systematically studied. However, this is a very complex issue that needs many further theoretical and experimental works in order to give a complete understanding.

TABLE II. Values of the characteristic parameters of the theory as from the master plot scaling procedure, the fit with the derivative of the KWW, and the fit with the derivative of the full β correlator.

	TTSP	KWW	Full β correlator
T_c (K)	229±3	227±5	230±3
λ	0.76±0.04	0.78±0.04	0.73±0.04

ACKNOWLEDGMENTS

We thank W. Götze, Th. Voigtmann, and F. Sciortino for very helpful suggestions and discussions, and for providing the computer program used to generate the full β correlator. This work was supported by the Commission of the European Communities through Contract No HPRI-CT1999-00111, by MURST cofin 2000, and by INFM through Project No. TREB-Sez.C-PAISS1999.

[1] U. Bengtzelius, W. Götze, and A. Sjölander, Solid State Phys. **17**, 5915 (1984); E. Leutheusser, Phys. Rev. A **29**, 2765 (1984); W. Götze, in *Liquids, Freezing and Glass Transition*, edited by J.P. Hansen, D. Levesque, and J. Zinn-Justin (North-Holland, Amsterdam, 1991), p. 287.

[2] R.V. Chamberlin, Phys. Rev. Lett. **82**, 2520 (1999).

[3] K.L. Ngai and R.W. Rendell, in *Supercooled Liquids. Advances and Novel Application*, edited by J.T. Fourkas, D. Kivelson, U. Mohanty, and K.A. Nelson (American Chemical Society, Washington, DC, 1996), p. 45.

[4] G. Li, W.M. Du, A. Sakai, and H.Z. Cummins, Phys. Rev. A **46**, 3343 (1992); W. Steffen, A. Patkowski, H. Glaser, G. Meier, and E.W. Fischer, Phys. Rev. E **49**, 2992 (1994); T. Franosch, W. Götze, M. Mayr, and A.P. Singh, *ibid.* **55**, 3183 (1997); J. Wuttke, J. Hernandez, G. Li, G. Coddens, H.Z. Cummins, F. Fujara, W. Petry, and H. Sillescu, Phys. Rev. Lett. **72**, 3052 (1994); G. Monaco, D. Fioretto, L. Comez, G. Ruocco, Phys. Rev. E **63**, 061502 (2001).

[5] U. Schneider, P. Lunkenheimer, R. Brand, and A. Loidl, Phys. Rev. E **59**, 6924 (1999); P. Lunkenheimer, U. Schneider, R. Brand, and A. Loidl, Contemp. Phys. **41**, 15 (2000).

[6] Y. Yang and K.A. Nelson, Phys. Rev. Lett. **74**, 4883 (1995).

[7] R. Torre, P. Bartolini, and R.M. Pick, Phys. Rev. E **57**, 1912 (1998).

[8] G. Hinze, R.S. Francis, and M.D. Fayer, J. Chem. Phys. **111**, 2710 (1999).

[9] A. Taschin, R. Torre, M. Ricci, M. Sampoli, C. Dreyfus, and R.M. Pick, Europhys. Lett. **53**, 407 (2001); R. Torre, A. Taschin, and M. Sampoli, Phys. Rev. E **64**, 061504 (2001).

[10] J. Wuttke, M. Ohl, M. Goldammer, S. Roth, U. Schneider, P. Lunkenheimer, R. Kahn, B. Ruffĺe, R. Lechner, and M.A. Berg, Phys. Rev. E **61**, 2730 (2000); M. Goldammer, C. Losert, J. Wuttke, W. Petry, F. Terki, H. Schober, and P. Lunkenheimer, *ibid.* **64**, 021303 (2001).

[11] L. Comez *et al.*, Phys. Rev. E **60**, 3086 (1999).

[12] R. Schilling and T. Scheidsteger, Phys. Rev. E **56**, 2932 (1997); T. Franosch, M. Fuchs, W. Götze, M.R. Mayr, and A.P. Singh, *ibid.* **56**, 5659 (1997); S. Kämmerer, W. Kob, and R. Schilling, *ibid.* **58**, 2141 (1998).

[13] R. Torre, M. Ricci, P. Bartolini, C. Dreyfus, and R.M. Pick, Philos. Mag. B **79**, 1897 (1999); R. Torre, P. Bartolini, M. Ricci, and R.M. Pick, Europhys. Lett. **52**, 324 (2000).

[14] G. Hinze, David D. Brace, S.D. Gottke, and M.D. Fayer, J. Chem. Phys. **113**, 3723 (2000); S.D. Gottke, David D. Brace, G. Hinze, and M.D. Fayer, J. Phys. Chem. B **105**, 238 (2001).

[15] W. Götze and L. Sjögren, Rep. Prog. Phys. **55**, 241 (1992);W. Götze, in *Liquids, Freezing and Glass Transition* (Ref. [1]), p. 287; W. Kob, in *Supercooled liquids. Advances and Novel Application* (Ref. [2]), p. 28; W. Götze, J. Phys.: Condens. Matter **11**, A1 (1999); H.Z. Cummins, *ibid.* **11**, A95 (1999).

[16] T. Franosch, M. Fuchs, W. Götze, M.R. Mayr, and A.P. Singh, Phys. Rev. E **55**, 7153 (1997).

[17] M. Ricci, P. Bartolini, and R. Torre, Philos. Mag. B **82**, 541 (2002).

[18] C. Alba-Simionesco and M. Krauzman, J. Chem. Phys. **102**, 6574 (1995).

[19] L. Sjögren, Phys. Rev. A **33**, 1254 (1986).

[20] T. Franosch, W. Götze, M.R. Mayr, and A.P. Singh, Phys. Rev. E **55**, 3183 (1997).

[21] W. Götze and Th. Voigtmann, Phys. Rev. E **61**, 4133 (2000).

[22] A. Aouadi, C. Dreyfus, M. Massot, R.M. Pick, T. Berger, W. Steffen, A. Patkowski, and C. Alba-Simionesco, J. Chem. Phys. **112**, 9860 (2000).

[23] D. Mc Morrow, W.T. Lotshaw, and G.A. Kenney-Wallace, IEEE J. Quantum Electron. **QE-24**, 443 (1988); W.T. Lotshaw, D. Mc Morrow, N. Thantu, J.S. Melonger, and R. Kitchenham, J. Raman Spectrosc. **26**, 571 (1995).

[24] R.W. Hellwarth, Prog. Quantum Electron. **5**, 1 (1977).

[25] Y. Yan and K.A. Nelson, J. Chem. Phys. **87**, 6240 (1987); **87**, 6257 (1987).

[26] P. Bartolini, M. Ricci, R. Torre, and R. Righini, J. Chem. Phys. **110**, 8653 (1999).

[27] S. Costantine, Y. Zhou, J. Morais, and L.D. Ziegler, J. Chem. Phys. **101**, 5456 (1997).

[28] W.M. Du, G. Li, H.Z. Cummins, M. Fuchs, J. Toulouse, and L.A. Knauss, Phys. Rev. E **49**, 2192 (1994).

[29] J. Wiedersich, N.V. Surovtsev, and E. Rossler, J. Chem. Phys. **113**, 1143 (2000).

[30] H.Z. Cummins, Gen Li, Weimen Du, Y.H. Hwang, and G.Q. Shen, Prog. Theor. Phys. Suppl. **126**, 21 (1997).

[31] S. Bovelli, D. Fioretto, and A. Jurlewicz, J. Phys.: Condens. Matter **13**, 373 (2000).

[32] S. Corezzi, S. Capaccioli, G. Gallone, M. Lucchesi, and P.A. Rolla, J. Phys.: Condens. Matter **11**, 10 297 (1999); D. Fioretto, A. Livi, P.A. Rolla, G. Socino, and L. Verdini, *ibid.* **6**, 5295 (1994); Y.Z. Wei and S. Sridhar, Rev. Sci. Instrum. **60**, 3041 (1989); K. Kremer and M. Arndt, in *Dielectric Spectroscopy of Polymeric Materials*, edited by J.P. Runt and J.J. Fitzgerald (American Chemical Society, Washington, DC, 1997), p. 67.

[33] C.J.F. Böttcher and P. Bordewijk, *Theory of Electric Polarisation* (Elsevier, Amsterdam, 1978), Vol. 2.

[34] C.P. Lindsey and G.D. Patterson, J. Chem. Phys. **73**, 3348 (1980).

[35] D. Favro, Phys. Rev. E **119**, 53 (1960); C.H. Wang, *Spectroscopy of Condensed Media, Dynamics of Molecular Interaction* (Academic Press, London, 1985); S. Dattagupta, *Relaxation Phenomena in Condensed Matter Physics* (Academic Press, London, 1987).

[36] E.N. Ivanov, Sov. Phys. JETP **18**, 1041 (1964).

[37] R. Pecora, *Dynamics Light Scattering* (Plenum, New York, 1985).